In silico characterization of cytisinoids docked into an acetylcholine binding protein

Juan Andrés Abin-Carriquiry [a,*], Margot Paulino Zunini [b,c], Bruce K. Cassels [d], Susan Wonnacott [e], Federico Dajas [a]

[a] Department of Neurochemistry, Instituto de Investigaciones Biológicas Clemente Estable, Av. Italia 3318, Montevideo, Uruguay
[b] LaBioFarMol, DETEMA, Facultad de Química, Universidad de la República, Montevideo, Uruguay
[c] Departamentos de Física y Química y Farmacia, Facultad de Ciencias, Universidad Católica del Norte, Antofagasta, Chile
[d] Department of Chemistry, Faculty of Sciences, University of Chile, Santiago, Chile
[e] Department of Biology and Biochemistry, University of Bath, Bath BA2 7AY, UK

ABSTRACT

Homology models of nicotinic acetylcholine receptors (nAChRs) suggest that subtype specificity is due to non-conserved residues in the complementary subunit of the ligand-binding pocket. Cytisine and its derivatives generally show a strong preference for heteromeric $\alpha 4 \beta 2^*$ nAChRs over the homomeric $\alpha 7$ subtype, and the structural modifications studied do not cause large changes in their nAChR subtype selectivity. In the present work we docked cytisine, *N*-methylcytisine, and several pyridone ring-substituted cytisinoids into the crystallographic structure of the *Lymnaea stagnalis* acetylcholine binding protein (AChBP) co-crystallized with nicotine (1UW6). The graphical analysis of the best poses showed that cytisinoids have weak interactions with the side chains of the non-conserved amino acids in the complementary subunit justifying the use of PDB 1UWB as a surrogate for nAChR. Furthermore, we found a high correlation ($R^2 = 0.96$) between the experimental pIC_{50} values at $\alpha 4 \beta 2^*$ nAChR and docking energy (S) of the best cytisinoid poses within the AChBP. Due to the quality of the correlation we suggest that this equation might be used as a predictive model to propose new cytisine-derived nAChRs ligands. Our docking results also suggest that further structural modifications of these cytisinoids will not greatly alter their $\alpha 4 \beta 2^* / \alpha 7$ selectivity.

© 2010 Elsevier Ltd. All rights reserved.

Neuronal nicotinic acetylcholine receptors (nAChRs) are widely distributed in the brain where they are involved in key central nervous system (CNS) functions such as cognition, motivation and motor activity, among others.[1–3] These receptors have been identified as promising targets for the treatment of several neurological disorders, such as Alzheimer's disease, Parkinson's disease, dyskinesias, Tourette's syndrome, schizophrenia, attention deficit disorder, anxiety and pain,[4–6] and development of subtype-selective nAChR ligands is a critical issue in this regard. Thus, the $\alpha 4 \beta 2$ nAChR, the most abundant subtype in the brain, is a major therapeutic target while the modulation of the $\alpha 3 \beta 4$ subtype is undesirable because it mediates cholinergic events in the autonomic nervous system.[7]

Cytisine is a plant alkaloid present in many species of the Fabaceae or Leguminosae that has higher affinity and specificity for $\alpha 4 \beta 2^*$ nAChRs than nicotine. It has been used as a template for the development of new nicotinic receptor ligands[4] and in fact varenicline, a cytisine analogue, was approved by the FDA in 2006

as an aid for smoking cessation, and cytisine itself has been used for this purpose for over forty years.[8] In previous studies we have shown that several structural substitutions can increase or decrease binding affinity and in vitro functional potency of cytisine. However, our studies also suggest that structural changes do not greatly affect the selectivity of these compounds for different nAChR subtypes.[9]

Structurally, nAChRs are homo- or heteropentamers forming a channel permeable to sodium and calcium ions, with an N-terminal ligand binding domain and a C-terminal transmembrane domain. The extracellular ligand binding domain contains a conserved disulfide pair that forms a so-called Cys-loop in each subunit. These domains form 2–5 binding sites at selected subunit interfaces. In response to the binding of two agonist molecules, a single ion channel is opened.[10] It has been very difficult to obtain detailed structural information about nAChRs and only the analysis of electron microscopy images has resulted in a 4-Å resolution model.[11] Better structural information about the nAChR ligand binding domains and the subunit interfaces has been obtained upon the discovery and crystallization of an acetylcholine binding protein from the snail *Lymnaea stagnalis* (Ls-AChBP),[12,13] a soluble

* Corresponding author. Tel./fax: +598 4872603.
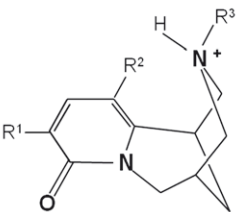*E-mail address:* abin@adinet.com.uy (J.A. Abin-Carriquiry).

homologue of the nAChR ligand binding domain in which the residues relevant for ligand binding are conserved also in the nAChR family. This crystal structure, and those obtained later for AChBP from other mollusks,[14] have proved most useful for analyzing the ligand binding domains, and several homology models of these proteins have been generated for different neuronal nAChR subtypes.[10,15–19]

The crystal structure of the Ls-AChBP–nicotine complex obtained by Celie (1UW6, DOI:10.2210/pdb1uw6/pdb) has illustrated the molecular contacts between the ligand and protein and is in excellent agreement with biochemical data obtained from nAChR binding studies.[20] This crystal structure shows in detail the agonist-receptor interaction for nicotine, and thus is an excellent template for small agonist-receptor interaction studies and, as we show here, for correlation studies of docking energy (S) versus experimentally measured affinity.

In this context, in the present work we have attempted to discover the structural determinants that give cytisinoids their ability to bind to nicotinic receptors and graphically understand how their structural differences are responsible for their different affinities. At the same time we identify which interactions with amino acids are most relevant in the binding site.

The tridimensional model of each cytisinoid shown in Chart 1 (cytisine, Cy; 3-bromocytisine, 3-BrCy; 3-iodocytisine, 3-ICy; N-methylcytisine, MCy; 3-bromo-N-methylcytisine, 3-BrMCy; 3,5-dibromocytisine, 3,5-diBrCy; 5-bromocytisine, 5-BrCy) was built as described in the Reference and notes section.[21] Chart 1 shows the 2D structure of each cytisine analogue as well as its biological activity (pIC50).[9]

Figure 1 shows all the contacts between the crystallographic structure of AChBP (1UW6) and the co-crystallized nicotine molecule. The contact distances were measured within a 4.5 Å radius sphere centered on the ligand.[22]

As described earlier,[23,24] ligands are completely buried within the protein at the interface between subunits (Fig. 1). The ligands make more direct contacts with the principal (+) side with residues from loops A, B and C than to the loops D, and E of the complementary (−) binding side, which are more variable regions among the different nAChRs subunits. Celie et al. estimated contact surfaces between nicotine and the amino acid residues on the principal (+) and complementary (−) sides of the binding site as approximately 75 and 50 Å^2, respectively.[20]

On the principal side, nicotine (as well as cytisine) makes extensive contacts with the side chain of Trp143 and some with Tyr192 and Tyr185, and cytisine also interacts with Thr144. The Tyr89 hydroxyl group has a close contact with the ligand, and the vicinal disulfide interacts, mostly through Cys188 (Figs. 1 and 2). On the complementary side, Trp53 makes limited aromatic contacts with nicotine (but not with cytisine). Met114 contributes with hydrophobic contacts to the binding of both ligands, while Leu112 only contributes in the case of nicotine.

In addition to these hydrophobic and aromatic contacts, two hydrogen bonds significantly contribute to the binding. The first hydrogen bond is between the nicotine pyridine N (or cytisine 2-pyridone carbonyl O) through a bridging water molecule to the main chain of residues Leu102 and Met114. The second hydrogen bond is between the nicotine pyrrolidine NH$^+$ and the carbonyl group of Trp143 or cytisine bispidine NH$_2^+$ and the OH group of Tyr89 (Figs. 1 and 2).

In particular, the charged nitrogen atoms of the ligands are in contact with an 'aromatic box' primarily consisting of the side chains of Tyr and Trp residues (Trp53, Trp143, Tyr185 and Tyr192) which form, mainly through Trp143 and Try185, a cation–π interaction.[18,25]

The use of the crystallographic coordinates of the AChBP for docking studies instead of a homology model for the α4β2 receptor is justified by the fact that all the amino acids that are important to establish contacts with the cytisinoids are the same in the mollusk protein and in the mammalian receptor, as is the case of Tyr89, Trp143, Thr144 Tyr185, Cys187, Cys188, Tyr192 in the alpha subunit. Even though the amino acids belonging to the complementary subunit are less conserved, the position of Trp53 remains constant. In the cases of the non-conserved residues, the main contributions to the binding energy arise through the backbone atoms, and mutations are not expected to have any great effect on the interaction. Leu102, Arg104 and Leu112 (Asp106, Val108 and Phe116 for α4β2 nAChRs, respectively) interact with ligands halogenated at C3 through main chain C=O and NH groups (see Table 1). In the case of Met114 and Leu118, the strongest interactions are through the carbonyl of the main chain so their mutation should not greatly affect their interaction with ligands. In summary, for all the cytisinoids studied, less than 10% of the weak interactions are not conserved in α4β2 nAChRs.

We used MOE Docking[26,27] in order to model the ligand binding to AChBP. To validate the docking results, the nicotine molecule was extracted from the X-ray structure of the nicotine–AChBP complex, subjected to the same calculations and conformational search as the cytisinoids, and re-docked into the AChBP. Figure 1 shows the superimposition of the three best scored nicotine poses at the binding site and the corresponding co-crystallized nicotine. The nicotine docking poses reproduce with high accuracy the position of nicotine in the crystal. The root mean square deviation (RMSD) between the experimental pose (in the crystal structure) and the best docked poses were 0.76, 0.54, 0.70, 0.51 and 0.39 Å^2 for the five binding sites, respectively (0.58 Å^2 average).[28]

Figure 2 shows, superimposed; the best scored poses of the seven cytisinoids docked into the binding site. Halogenation at C5 (5-BrCy; 3,5-diBrCy) produces repulsive van der Waals interactions with the receptor, given the proximity of the C5 halogen atom
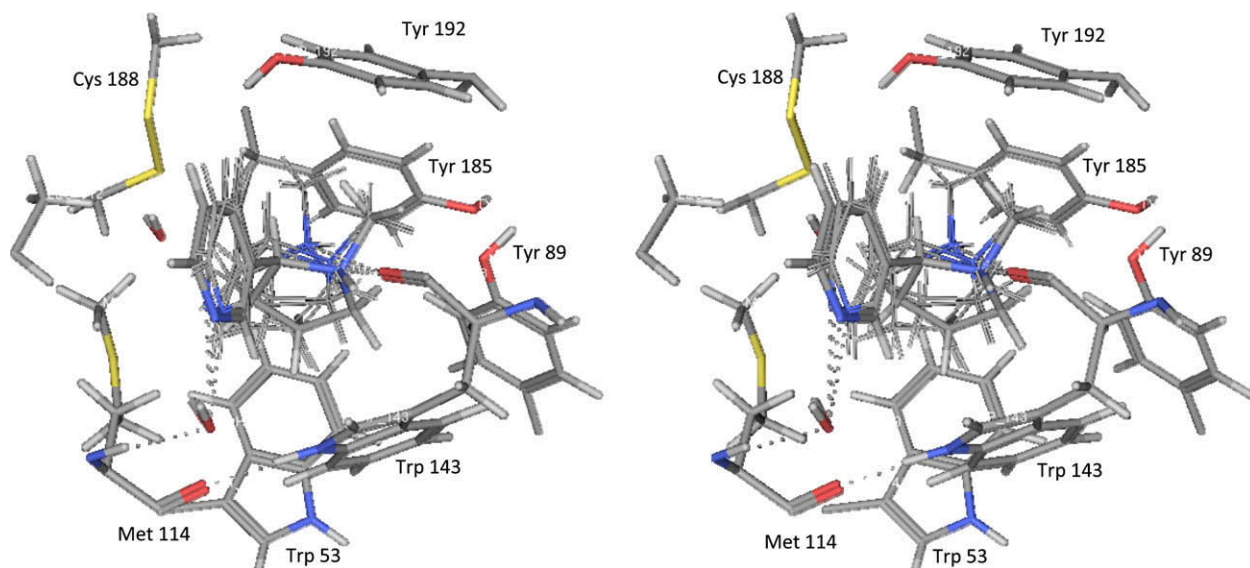

Ligand	Substitutions			[³H]epibatidine binding site
	R^1	R^2	R^3	pIC$_{50}$ ± S.E.M. (M)
Cy	H	H	H	9.05 / 7.16
3-BrCy	Br	H	H	9.51 ± 0.05
3-ICy	I	H	H	9.61 ± 0.05
MCy	H	H	CH$_3$	6.95 ± 0.07
3-BrMCy	Br	H	CH$_3$	6.99 ± 0.08
3,5-diBrCy	Br	Br	H	6.43 ± 0.06
5-BrCy	H	Br	H	6.34 ± 0.03

Chart 1. Experimental binding affinities (pIC$_{50}$) of the docked compounds.[6]

Figure 1. Superimposition of the crystallographic (bars) and the three best docked poses (sticks) of nicotine inside the binding site of the AChBP PDB 1UW6.
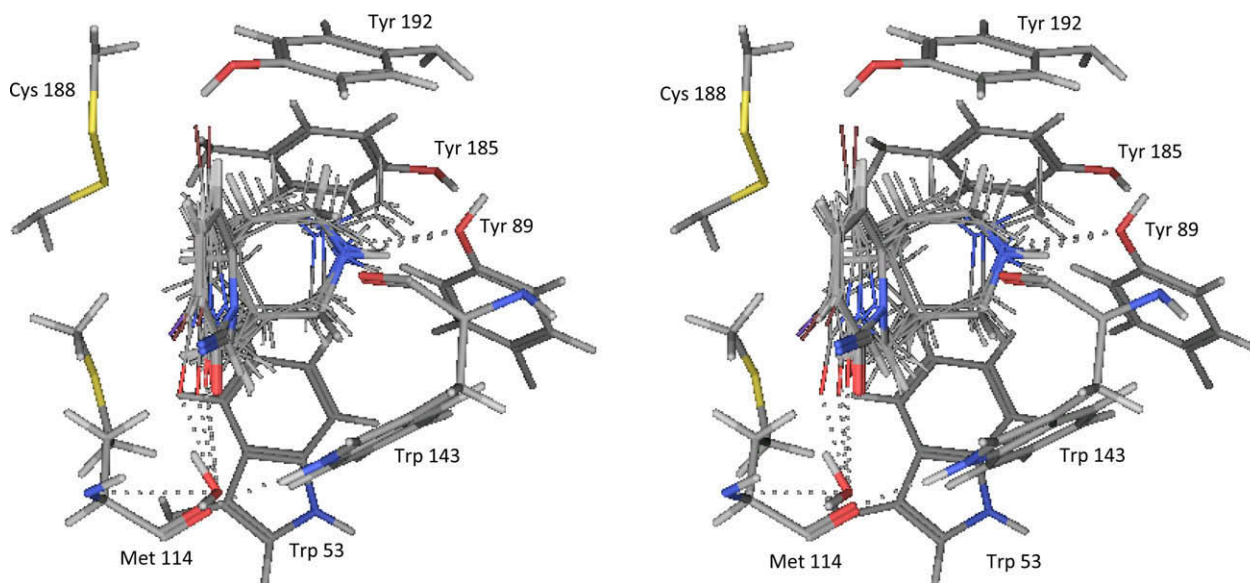

Figure 2. Superimposition of the best docked poses of the different cytisinoids studied inside the binding site of the AChBP PDB 1UW6.

Table 1
Number of contacts (mean of the five binding sites ± standard deviation) between *Lymnaea stagnalis* AChBP amino acids and ligands. The second column shows the putative amino acid at the rat α4β2 nAChR subtype

AChBP	α4β2	3-BrCy	3-Icy	Cy	3-BrMCy	MCy	3,5-diBrCy	5-BrCy
Tyr89	Tyr91	7 ± 1	6 ± 0	6 ± 0	9 ± 2	10 ± 1	6 ± 0	5 ± 2
Arg104	Val108	1 ± 1	1 ± 1	0 ± 0	5 ± 3	0 ± 0	0 ± 0	0 ± 0
Leu112	Leu116	2 ± 1	2 ± 1	0 ± 0	7 ± 4	0 ± 0	0 ± 0	0 ± 0
Met114	Leu118	27 ± 1	27 ± 2	27 ± 1	30 ± 2	30 ± 1	28 ± 1	28 ± 2
Trp143	Trp148	39 ± 1	39 ± 1	40 ± 2	35 ± 5	38 ± 0	37 ± 2	39 ± 3
Thr144	Thr148	8 ± 1	9 ± 1	3 ± 2	11 ± 2	5 ± 3	8 ± 2	5 ± 3
Tyr185	Tyr189	13 ± 3	12 ± 3	12 ± 2	17 ± 2	18 ± 2	11 ± 1	10 ± 2
Cys187	Cys191	3 ± 1	3 ± 1	4 ± 1	4 ± 1	5 ± 2	5 ± 1	6 ± 3
Cys188	Cys192	2 ± 1	2 ± 1	2 ± 1	2 ± 1	3 ± 0	6 ± 1	5 ± 1
Tyr192	Tyr196	18 ± 1	18 ± 2	18 ± 2	20 ± 4	21 ± 3	24 ± 2	25 ± 3
Total number of contacts		124 ± 3	123 ± 2	112 ± 5	142 ± 5	130 ± 4	128 ± 4	122 ± 4

Table 2

Distances (Å) between the most relevant interacting ligand atoms and Ls-AChBP atoms (mean of the five binding sites ± standard deviation) or % of HB score (mean ± standard deviation)

Interaction		3-BrCy	3-ICy	Cy	3-BrMCy	MCy	3,5-diBrCy	5-BrCy
Ligand	AChBP							
H^+	OH-Tyr 89	2.0 ± 0.1	2.2 ± 0.2	2.0 ± 0.1	-	-	2.1 ± 0.2	2.4 ± 0.2
HB Score (%)		41 ± 8%	47 ± 15%	50 ± 16%			42 ± 20%	36 ± 10%
O Carbonyl	HOH	2.7 ± 0.2	2.7 ± 0.2	2.8 ± 0.2	2.4 ± 0.2	2.5 ± 0.1 A	2.8 ± 0.2	2.9 ± 0.3
HB Score (%)		65 ± 20%	68 ± 17%	58 ± 27%	55 ± 15%	73 ± 12%	50 ± 32%	56 ± 28%
Total HB Score (%)	107 ± 20%	114 ± 13%	108 ± 14%	55 ± 15%	73 ± 12%	92 ± 28%	92 ± 20%	—
3 Hal	O-Leu102	4.0 ± 0.4	4.0 ± 0.5	—	>4.5	—	>4.5	—
3 Hal	N-Arg104	3.9 ± 0.3	3.7 ± 0.1	—	3.3 ± 0.5	—	>4.5	—
3 Hal	O-Leu112	3.5 ± 0.1	3.4 ± 0.1	—	3.0 ± 0.3	—	4.1 ± 0.3	—
3 Hal	N-Met114	4.4 ± 0.1	4.4 ± 0.1	—	4.3 ± 0.2	—	>4.5	—
3 Hal	Cg-Thr144	3.5 ± 0.2	3.5 ± 0.2	—	4.0 ± 0.3	—	3.1 ± 0.2	—
3 Hal	Cp-Thr144	3.9 ± 0.1	3.9 ± 0.1	—	4.3 ± 0.2	—	3.4 ± 0.1	—
5 Hal	OH-Tyr192	—	—	—	—	—	1.8 ± 0.1	1.7 ± 0.1
5 Hal	S-Cys188	—	—	—	—	—	2.6 ± 0.2	2.7 ± 0.2

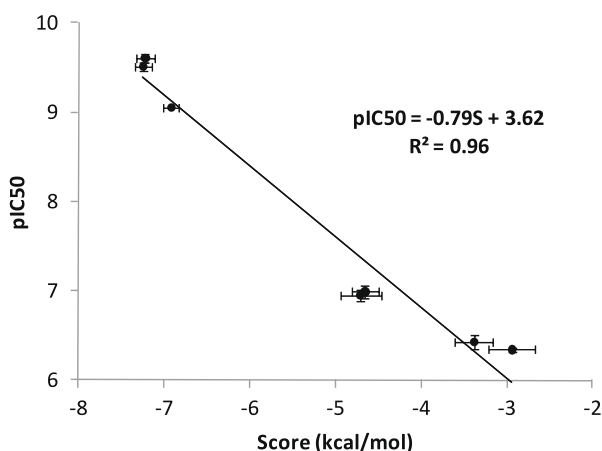**Figure 3.** Correlation between experimental cytisinoid pIC_{50} values at rat α4β2 nAChRs versus the calculated interaction energies (S, kcal/mol) of their complexes with AChBP 1UW6. Bars represent standard errors.

to Cys188 and Tyr192. Consequently, these substituted cytisinoids are slightly re-located, causing a decrease in the contribution of the hydrogen bonds (see Table 2).

N-methylation (MCy, 3-BrMCy) hinders the formation of a H-bond with the Tyr89 OH group, while reinforcing the hydrogen bond between the cytisine 2-pyridone carbonyl O through a bridging water molecule to the backbone NH of residues Leu102 and Met114, but the greater strength of the latter interaction is not enough to offset the loss of the former one (see Table 2).

Finally, halogenation at C3 (3-BrCy, 3-ICy, 3-BrMCy) favours interactions with the backbone O of Leu102, backbone N of Arg104, backbone O of Leu112, backbone N of Met114 and Cγ and Cβ of Thr144, while the H-bonds with the OH group of Tyr89 and a water molecule remain constant (see Table 2).

Because the AChBP is a homopentamer, there are five identical binding sites. For each site, docking was performed three times and the best scored poses were retrieved and averaged. Then the five averaged scores, one for each binding site, were averaged again. These averages were correlated with the experimental affinities (IC_{50}) as shown in Figure 3. Two binding pIC_{50} values have been reported for cytisine, which has higher affinity for the α4(non α6)β2* subtype, and lower for α6β2*.[29,30] In order to calculate the correlation we use the one associated with α4(non α6)β2*.

Figure 3 shows the correlation between the experimental affinities (pIC_{50}) and energies (scores) resulting from cytisinoid-receptor docking. The R^2 value of 96% obtained suggests that, within the cytisinoid series, and if all compounds adopt similar docking poses, the docking scores might be useful to predict activity and propose new designs (Eq. 1):

$$pIC_{50} = -0.79S + 3.62 \tag{1}$$

Because the score was calculated in triplicate for each of the five compounds, and in view of the small standard deviations shown in Figure 3, one can conclude that this result has an appropriate level of precision.

In the present work, we have validated a simulation procedure (docking) which can precisely predict the most probable nicotine pose into each binding site of the AChBP, using the PDB 1UW6 model as a template. Using this validated procedure we can predict how cytisine interacts with these binding sites. Furthermore, after docking simulations, we find that the most stable poses of the different cytisinoids studied are quite similar to each other. Moreover, the cytisinoid poses at the binding sites are highly reproducible, and consequently their scores are very precise (low coefficient of variation). The graphical analysis of our docking results for the different cytisinoids, together with their theoretical binding energies (scores), are clearly related to the experimental conclusion that N-methylation and substitution at C5 are unfavourable, whereas halogenation at C3 is favourable for binding to α4β2 nAChRs. In our view, this indicates that a computational model of L. stagnalis AChBP is a good approximation to explain the affinities of these cytisinoids for the rat α4β2 nAChR.

Finally, as docking experiments have shown, cytisinoids interact primarily with the major component, and to a lesser extent with the complementary component of the receptor binding site. The high degree of conservation of the main chain at the site of contact and a relatively minor interaction with the side chains of the 'mutated' amino acid residues of the complementary site reasonably justify the choice of the crystallographic structure of AChBP (1UW6) as a template for α4β2 nAChR. This minor interaction of cytisinoids with the complementary site could also explain why structural modifications on the cytisine scaffold do not lead to large changes in their α4β2*/α7 selectivity.

One of the main achievements of this study is an equation that links the docking energy (score) and the experimental pIC_{50} values with a very strong correlation ($R^2 = 0.96$). We can therefore conclude that this equation should be useful for the prediction of affinities of cytisinoids that have not been considered in the study sample but share the same binding mode, and consequently, to design new molecules that could be synthesized and for which we can estimate their pIC_{50} values in advance.

Acknowledgements

References and notes

1. Wonnacott, S.; Barik, J.; Dickinson, J.; Jones, IW. *J. Mol. Neurosci.* **2006**, *30*, 137.
2. Newhouse, P. A.; Singh, A.; Potter, A. *Curr. Top. Med. Chem.* **2004**, *4*, 267.
3. Newhouse, P. A.; Potter, A.; Singh, A. *Curr. Opin. Pharmacol.* **2004**, *4*, 36.
4. Cassels, B. K.; Bermúdez, I.; Dajas, F.; Abin-Carriquiry, J. A.; Wonnacott, S. *Drug Discovery Today* **2005**, *10*, 1657.
5. Lloyd, G. K.; Williams, M. *J. Pharmacol. Exp. Ther.* **2000**, *292*, 461.
6. Hogg, R. C.; Bertrand, D. *Curr. Drug Targets CNS Neurol. Disord.* **2004**, *3*, 123.
7. Yuan, H.; Petukhov, P. A. *Bioorg. Med. Chem.* **2006**, *14*, 7936.
8. Tutka, P. *Expert Opin. Investig. Drugs* **2008**, *17*, 1473.
9. Abin-Carriquiry, J. A.; Voutilainen, M. H.; Barik, J.; Cassels, B. K.; Iturriaga-Vásquez, P.; Bermudez, I.; Durand, C.; Dajas, F.; Wonnacott, S. *Eur. J. Pharmacol.* **2006**, *536*, 1.
10. Le Novère, N.; Grutter, T.; Changeux, J. P. *Proc. Natl. Acad. Sci. U.S.A.* **2002**, *99*, 3210.
11. Unwin, N. *J. Mol. Biol.* **2005**, *346*, 967.
12. Brejc, K.; van Dijk, W. J.; Smit, A. B.; Sixma, T. K. *Nature* **2001**, *411*, 269.
13. Smit, A. B.; Syed, N. I.; Schaap, D.; van Minnen, J.; Klumperman, J.; Kits, K. S.; Lodder, H.; van der Schors, R. C.; van Elk, R.; Sorgedrager, B.; Brejc, K.; Sixma, T. K.; Geraerts, W. P. *Nature* **2001**, *411*, 261.
14. Celie, P. H.; Klaassen, R. V.; van Rossum-Fikkert, S. E.; van Elk, R.; van Nierop, P.; Smit, A. B.; Sixma, T. K. *J. Biol. Chem.* **2005**, *280*, 26457.
15. Henchman, R. H.; Wang, H. L.; Sine, S. M.; Taylor, P.; McCammon, J. A. *Biophys. J.* **2003**, *85*, 3007.
16. Sullivan, D.; Chiara, D. C.; Cohen, J. B. *Mol. Pharmacol.* **2002**, *61*, 463.
17. Schapira, M.; Abagyan, R.; Totrov, M. *BMC Struct. Biol.* **2002**, *2*, 1.
18. Artali, R.; Bombieri, G.; Meneghetti, F. *Farmaco* **2005**, *60*, 313.
19. Costa, V.; Nistri, A.; Cavalli, A.; Carloni, P. *Br. J. Pharmacol.* **2003**, *140*, 921.
20. Celie, P. H.; van Rossum-Fikkert, S. E.; van Dijk, W. J.; Brejc, K.; Smit, A. B.; Sixma, T. K. *Neuron* **2004**, *41*, 907.
21. The geometries of the protonated ligands were optimized using the MMFF94 molecular mechanics forcefield function in MOE, and then refined using the PM3 quantum chemical model implemented in MOPAC, with a convergence criterion of 0.0005 kcal mol^{-1} for energy. (a) Gill, P.; Murray, W.; Wright, M. *Practical Optimization*; Academic Press: London, 1981; (b) Stewart, J. J. P. MOPAC Manual, 7th ed., 1993.; (c) Beusen, D. D.; Berkley Shands, E. F.; Karasek, S. F.; Marshall, G. R.; Dammkoehler, R. A. *J. Mol. Struct. THEOCHEM.* **1996**, *370*, 157.
22. The edited crystal structure (water molecules included) of the AChBP (PDB 1UW6) was imported into MOE and all hydrogen atoms were added to the structure with their standard geometry. The hydrogens corresponding to the crystallographic water near the pyridine nitrogen of each nicotine were manually redirected in order to obtain a model with hydrogen bonds between them and Leu102 and Met114 as described by Celie et al. After manually placing each water molecule and guiding it to form the required hydrogen bonds, a local energy minimization of the molecule was performed. The sequences of AChBP and extracellular ligand binding domains (LBDs) of the different subunits were aligned using CLUSTALW 2. We chose to do a full alignment, with a sequence format FASTA (Pearson) measuring the score type as a percentage, without end gaps. All other parameters (KTUP, window length, topdiag, pair gap, matrix, gap open, gap extension and gap distance) were set with the default definitions given in the web site. Similar results were obtained by Le Novère et al. (2002). (a) Cheatham, T. E., 3rd; Brooks, B.R.; Kollman, P.A. *Curr. Protoc. Nucleic Acid Chem.* **2001**, Chapter 7. Unit 7 9. (b) Thompson, J. D.; Gibson, T. J.; Plewniak, F.; Jeanmougin, F.; Higgins, D. G. *Nucleic Acids Res.* **1997**, *25*, 4876. (c) Mackey, A. J.; Haystead, T. A.; Pearson, W. R. *Mol. Cell. Proteomics.* **2001**, *1*, 139. (d) Larkin, M. A.; Blackshields, G.; Brown, N. P.; Chenna, R.; McGettigan, P. A.; McWilliam, H.; Valentin, F.; Wallace, I. M.; Wilm, A.; Lopez, R.; Thomson, J. D.; Gibson, T. J.; Higgins, D. G. *Bioinformatics* **2007**, *23*, 2947. Higgins, D.; Thompson, J.; Gibson, T.; Thompson, J. D.; Higgins, D. G.; Gibson, T. J. *Nucleic Acids Res.* **1994**, *22*, 4673. (e) Lopez, R. Services Programme and Loyd A. (1997) http://www.ebi.ac.uk/Tools/clustalw2/.
23. Sine, S. M. *J. Neurobiol.* **2002**, *53*, 431.
24. Karlin, A. *Nat. Rev. Neurosci.* **2002**, *3*, 102.
25. Xiu, X.; Puskar, N. L.; Shanata, J. A.; Lester, H. A.; Dougherty, D. A. *Nature* **2009**, *458*, 534.
26. MOE (The Molecular Operating Environment), Version 2006.08, software available from Chemical Computing Group Inc., 1010 Sherbrooke Street West, Suite 910, Montreal, Canada H3A 2R7, http://www.chemcomp.com).
27. Labute, P. Probabilistic Receptor Potentials. Journal of the Chemical Computing Group; http://www.chemcomp.com/journal/cstat.htm, 2001.
28. We validated the procedure by taking the coordinates of the nicotine molecule obtained from the 1UW6 crystal structure and docking it into the model of the apoprotein. As the 'receptor' we used all the crystallographic coordinates of 1UW6, with the nicotine removed. The validation protocol consisted of: (a) carrying out a fit of each one of the nicotine conformations obtained from a conformational database, (b) taking as 'receptor' the ensemble of protein and solvent atoms, (c) determining as 'site' the set of all atoms within a sphere of 4.5 Å centered at the nicotine molecule in the 1uw6 crystal, (d) using the ligand conformational data base obtained in the previous stage without an additional conformational search, (e) using the alpha PMI placement system and (f) calculating the interaction free energy dG by using the affinity dG scoring function.
Cytisinoid–AChBP docking: for each ligand at each binding site, a molecular database with 100 docked conformations was obtained. The poses of each ligand were already ranked according to the best score (kcal/mol). For each ligand the higher *S* values were retrieved at each binding position. The procedure was repeated three times and the best score values were averaged.
29. Zoli, M.; Léna, C.; Picciotto, M. R.; Changeux, J. P. *J. Neurosci.* **1998**, *18*, 4461.
30. Whiteaker, P.; Jimenez, M.; McIntosh, J. M.; Collins, A. C.; Marks, M. J. *Br. J. Pharmacol.* **2000**, *131*, 729.